A Microscopic Model for the Fluctuations of Local Field and Spontaneous Emission of Single Molecules in Disordered Media

Renaud A. L. Vallée,*[a] Mark Van Der Auweraer,[a] Frans C. De Schryver,[a] David Beljonne,[b] and Michel Orrit[c]

We develop a microscopic model to describe the observed temporal fluctuations of the fluorescence lifetime of single molecules embedded in a polymer at room temperature. The model represents the fluorescent probe and the macromolecular matrix on the sites of a cubic lattice and introduces voids in the matrix to account for its mobility. We generalize Lorentz's approach to dielectrics by considering three domains of electrostatic interaction of the probe molecule with its nanoenvironment: 1) the probe molecule with its elongated shape and its specific polarizability, 2) the first few solvent shells with their discrete structure and their inhomogeneity, 3) the remainder of the solvent at larger distances, treated as a continuous dielectric. The model is validated by comparing its outcome for homogeneous systems with those of existing theories. When realistic inhomogeneities are introduced, the model correctly explains the observed fluctuations of the lifetimes of single molecules. Such a comparison is only possible with single-molecule observations, which provide a new access to local field effects.

1. Introduction

While the interaction of electromagnetic fields with single molecules is well understood in vacuum,[1] the situation is much more complex in condensed phases: the presence of polarizable media considerably alters the quantum fluctuation properties of the fields.[2] Most approaches consider the electromagnetic field as a macroscopic field modified by the local field factor, which takes into account the effect of the nanosurrounding of the probe molecule. On the one hand, the validity of the old but still frequently used Lorentz field factor continues to be investigated.[3] On the other hand, Glauber et al.[2] derived an expression (empty cavity factor) for the spontaneous emission of an excited probe located within a uniform medium of dielectric constant ε. This expression was also derived and checked experimentally by Yablonovitch et al.[4] Recently, it was shown that the empty cavity factor applies for a substitutional probe while the Lorentz cavity factor applies for an interstitial probe (the probe is inserted without displacement of the matrix molecules).[5] However, these approaches consider a uniform surrounding, such that the influence of the discrete structure of nearby molecules on the probe molecule averages out. The local, inhomogeneous nature of the medium is neglected. The local dielectric properties play an important role in the structure and functionality of proteins.[6,7,8] A more microscopic picture of the local effects has to be considered. Due to its intrinsic ability to sense the nanosurrounding of a probe molecule,[9] single-molecule spectroscopy constitutes the ideal tool to perform this task. A first step forward has been accomplished in this respect by Donley et al., who reported on the observation of radiative lifetime distributions of single terrylene molecules embedded in polyethylene at a temperature of 30 mK.[10]

In a recent publication,[11] Vallée et al. reported on the temporal fluorescence lifetime fluctuations of DiD (1,1-dioctadecyl-3,3,3′,3′-tetramethylindodicarbocyanine) single molecules (Scheme 1) embedded in diverse polymer matrices frozen in

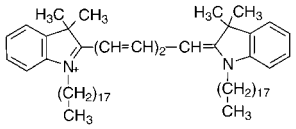

Scheme 1. *Chemical structure of a DiD molecule.*

the glassy state. The lifetime fluctuations were attributed to a fluctuating density of the polymer segments surrounding the nanoprobe. A polymer matrix is a highly disordered and inhomogeneous system that, according to hole theories,[12,13] may be seen as an ensemble of polymer segments and holes allowed to move on a lattice. In the frame of an effective medium theory, the fluctuating hole configuration was described by a fluctuating dielectric constant around each single

[a] *Dr. R. A. L. Vallée, Prof. Dr. M. Van Der Auweraer, Prof. Dr. F. C. De Schryver*
Laboratory for Spectroscopy and Photochemistry
Catholic University of Leuven, Celestijnenlaan 200 F
3001 Leuven (Belgium)
Fax: (+32) 16-32-7990
E-mail: renaud.vallee@chem.kuleuven.ac.be

[b] *Dr. D. Beljonne*
Laboratory for Chemistry of Novel Materials
University of Mons, Place du Parc 20, 7000 Mons (Belgium)

[c] *Prof. Dr. M. Orrit*
Huygens Laboratory, P.O. Box 9504
2300 RA Leiden (The Netherlands)

 DOI: 10.1002/cphc.200400439

molecule.[14] The asymmetric fluorescence lifetime distribution for each individual molecule was related in this way to a corresponding distribution of holes surrounding the probe molecule. Consequently, a characteristic number of segments involved in a rearrangement cell around each individual molecule was determined. Interestingly, the shape of the fluorescence lifetime distributions, and consequently the number of segments involved in a rearrangement volume around the probe molecule, was found to decrease with increasing temperature.

Powerful though this model proved to be in interpreting the data, it presents several interrelated drawbacks. Firstly, the microscopic structure of the probe molecule is completely neglected: by using a spherical empty cavity factor[15] in the calculation of the fluorescence lifetime, the probe molecule has been considered as being of spherical shape and nonpolarizable.[11] In most treatments of local fields in dielectrics, a Lorentz factor is used. This assumes that a spherical molecule is placed in a isotropic, homogeneous medium.[3] In addition, the polarizability of the probe is taken equal to that of the matrix. In this work, we wish to go beyond these assumptions. We will consider 1) the elongated shape of the DiD molecule (Scheme 1),[16] 2) the actual polarizability of its conjugated system, which is much larger than that of the surrounding monomer units, 3) the microscopic structure of the first solvent shells around the probe, possibly including inhomogeneities.

This paper further explores the previous approach and provides a full microscopic interpretation of the lifetime fluctuations. The optical and structural properties of the individual molecule and of the surrounding monomer units are determined by quantum-chemical calculations. As the interaction between them is limited to a few nanometers, that is, is much smaller than the radiative emission wavelength $\lambda = 660$ nm, only nonretarded electrostatic interactions will be taken into account in the description.

2. Local Field in the Continuum Approach

Figure 1a shows the fluorescence-lifetime time trace of a DiD single molecule embedded in a poly(styrene) (PS, $M_w = 133\,000$, polydispersity index $= 1.06$) matrix. While the lifetime has an average value of $\tau = 2.1$ ns, it deviates frequently and asymetrically towards higher values during the experiment. The fluorescence lifetime fluctuations of the individual molecule can be as large as 30% with respect to the average value, as best represented by the corresponding distribution shown in Figure 1b.

The spontaneous emission rate Γ_{r0} of a single fluorescent molecule in vacuum is given by the Einstein A_{eg} coefficient for emission in Equation (1):

$$\Gamma_{r0} = A_{eg} = \frac{1}{\tau_0} = \frac{4}{3}\frac{|\vec{\mu}_{eg}|^2}{4\pi\varepsilon_0\hbar}\left(\frac{\omega_{eg}}{c}\right)^3 \quad (1)$$

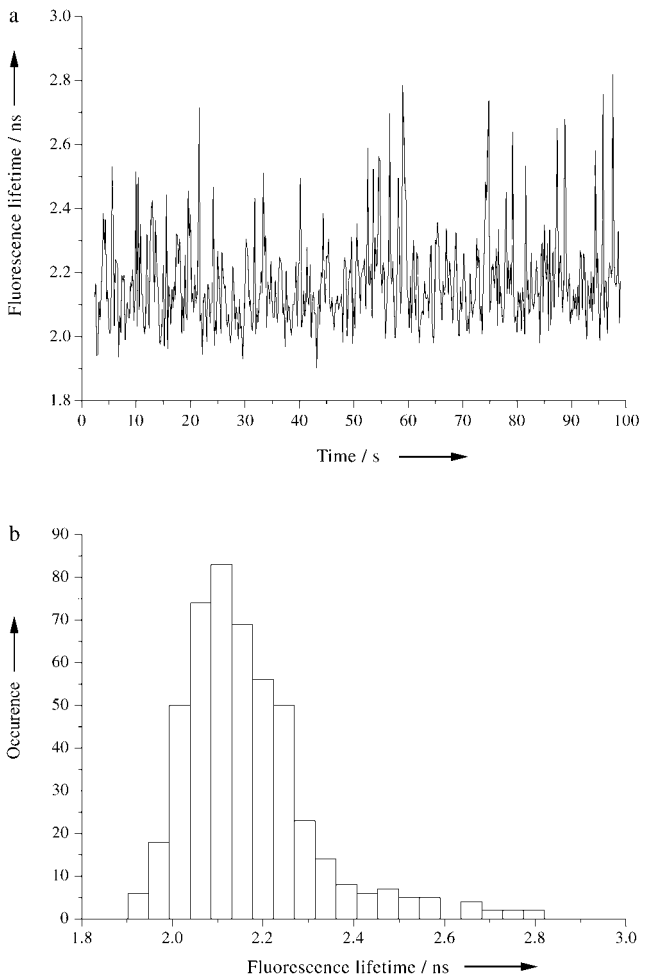

Figure 1. *Fluorescence lifetime time trajectory (a) and distribution (b) of a single DiD molecule embedded in a PS film.*

where $\vec{\mu}_{eg}$ and ω_{eg} are the transition dipole moment and transition frequency of the molecule, respectively; ε_0 is the dielectric permittivity of vacuum, $\hbar$ is the reduced Planck constant and c is the speed of light in vacuum. τ_0 is the inherent radiative lifetime of the molecule. This observable is an intrinsic property of the probe molecule. While this is indeed true in vacuum, the lifetime of the probe molecule strongly depends on its direct environment, and in particular on the dielectric properties of the medium in which it is embedded. In a transparent condensed medium of relative dielectric permittivity (high-frequency part), the energy of the emitted photon is renormalized through the substitutions $\varepsilon_0 \rightarrow \varepsilon_r\varepsilon_0$ and $c \rightarrow c/n$, such that the spontaneous emission rate can be written as Equation (2):

$$\Gamma_r = n\Gamma_{r0} \quad (2)$$

where $n = \sqrt{\varepsilon_r}$ is the refractive index of the considered medium ($n = 1.58$ in the case of PS). Nienhuis et al.[17] firstly derived this formula by quantizing the macroscopic Maxwell equations.

It is worthwhile to mention here that the actual fluorescence lifetime of a single molecule embedded in a real medium results from both radiative (rate Γ_r) and nonradiative (rate Γ_{nr}) processes [Eq. (3)]:

$$\tau_f = \frac{1}{\Gamma_r + \Gamma_{nr}} \quad (3)$$

so that the opening of decay channels other than radiative can modify the lifetime. The quantum yield $\eta = \frac{\Gamma_r}{\Gamma_r+\Gamma_{nr}}$ of the DiD molecule has been shown to be very close to unity, which makes extra—nonradiative—decay channels irrelevant for the system under consideration.[11] In the remaining of this paper, we will only consider variations of the radiative rate.

The complex nature of the interaction of the probe molecule-surrounding dielectric, involving discrete and continuous parts, will be described by considering three separate domains (Figure 2): 1) the molecule with its elongated shape and specif-

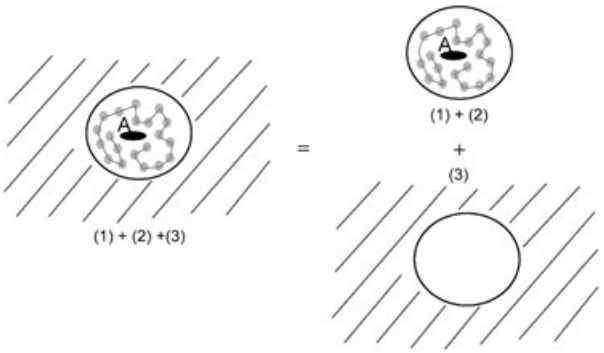

Figure 2. *Description of the system under investigation: the probe molecule A (1) and its first few solvent shells (2) are considered with their discrete structure and embedded in the remainder of the matrix treated as a continuum (3).*

ic polarizability, 2) the first few solvent shells with their discrete structure and their possible inhomogeneity, 3) the remainder of the solvent at long distances, treated as a continuum.

The molecule and the first solvent shells will be treated exactly by means of simulations given in Section 3. In this section, we replace them by one dipole at the center of a dielectric sphere with the same polarizability as the surroundings. We then reinsert this sphere into the dielectric, à la Lorentz, applying the relevant local field factor.

2.1 Lorentz Cavity Factor

We first consider a homogeneous, isotropic medium of identical molecules. Because of the relatively close proximity of the atoms or molecules in condensed phases, the local field $\vec{E}_l$ felt by the probe molecule can be very different from the applied electric field $\vec{E}_{ap}$. Figure 3 shows a two-dimensional representation of the Lorentz virtual spherical cavity model: a molecule A of the medium is surrounded by an imaginary sphere (represented by the circle) of such extent that beyond it the dielectric can be treated as a continuum.

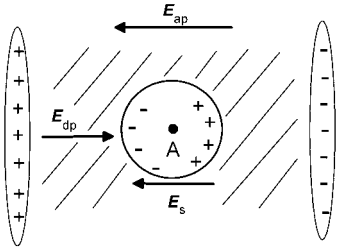

Figure 3. *Two-dimensional representation of the Lorentz model.*

When a field $\vec{E}_{ap}$ is applied to the sample (represented by the rectangle), charges accumulate on its surface in response to $\vec{E}_{ap}$. A depolarizing field $\vec{E}_{dp}$ is established, that opposes to $\vec{E}_{ap}$, thus lowering the net electrostatic field in the sample. The resultant macroscopic field $\vec{E}_m$ is then simply the sum $\vec{E}_{ap}+\vec{E}_{dp}$. Taking into account the discontinuous atomic or molecular nature of the dielectric within the sphere centered on the probe molecule A (but treating the region outside the sphere as a continuum), $\vec{E}_l$ can be written as Equation (4):

$$\vec{E}_l = \vec{E}_m + \vec{E}_s + \vec{E}_d \quad (4)$$

where $\vec{E}_s = \frac{\varepsilon-1}{3}\vec{E}_m$ is the contribution of the charges at the surface of the sphere. $\vec{E}_d$ is due to the dipoles within the sphere, near to A, and must be calculated for each particular site and for each dielectric material as it depends strongly on the geometrical arrangement and polarizability of the contributing particles. When the molecules surrounding A are neutral, nonpolar molecules, or when they are arranged either in complete disorder or in a cubic lattice, the assumption (proved by Lorentz in the case of a cubic arrangement of identical molecules) is often made that the additional effects of these molecules on the probe molecule mutually cancel, such that $\vec{E}_d = \vec{0}$. The Lorentz local field factor L_L, which relates the microscopic local electric field to the macroscopic electric field $E_l = L_L\vec{E}_m$, is thus simply given by Equation (5):[18]

$$L_L = \frac{\varepsilon+2}{3} \quad (5)$$

2.2 Effect of the Molecular Polarizability—Reaction Field

We now consider a probe molecule with a spherical shape but a specific polarizability. In a medium of polarizability α and dielectric constant ε relative to vacuum, a small volume is now replaced by the molecule A of interest: we model it by a point dipole $\vec{\mu}$ with polarizability χ, placed at the center of a spherical cavity. The field of the dipole in such a cavity polarizes the surrounding molecules, and the resulting inhomogeneous polarization of this nanoenvironment gives rise to the reaction field $\vec{E}_r$ acting at the position of the dipole. For symmetry reasons, the reaction field $\vec{E}_r$ has the same direction as the original dipole moment $\vec{\mu}$ and is proportional to $\vec{\mu}$ as long as no saturation effects occur: $\vec{E}_r = f\vec{\mu}$.[18] As the molecule is placed in a spherical cavity of radius R, a simple consideration of the

continuity of the fields inside and outside the cavity leads to Equation (6) for the cavity field $\vec{E}_c$ (local field in the center):

$$\vec{E}_c = \frac{3\varepsilon}{2\varepsilon+1}\vec{E}_m \quad (6)$$

The local field felt by the molecule $\vec{E}_l = \vec{E}_c + \vec{E}_r$ is the sum of the cavity field and the reaction field, such that [Eq. (7)]:

$$\vec{E}_l = \vec{E}_c \frac{1}{1-f\chi} \quad (7)$$

where f writes as given in Equation (8):

$$f = 2\frac{\varepsilon-1}{2\varepsilon+1}\frac{1}{4\pi\varepsilon_0 R^3} \quad (8)$$

By combining Equations (6–8), the local field factor L that relates the local field effectively felt by the molecule to the macroscopic electric field becomes [Eq. (9)]:

$$L = \frac{3\varepsilon}{2\varepsilon+1-2(\varepsilon-1)\frac{\chi}{4\pi\varepsilon_0 R^3}} \quad (9)$$

In the special case where the molecule at the center has the polarizability α of the medium, we must recover Lorentz's theory of dielectrics. Inserting in Equation (9) the well-known Clausius–Mossotti relation in the slightly modified form [Eq. (10)]:

$$V = \frac{\alpha}{\varepsilon_0}\frac{\varepsilon+2}{3(\varepsilon-1)} \quad (10)$$

where $V = 4/3\,\pi R^3$ is the volume occupied by a single spherical molecule, one indeed finds back the Lorentz local field factor given by Equation (5). In the general case, $\chi = \alpha + \delta$, where δ is the polarizability difference of the molecule with respect to the medium. The local field factor [Eq. (11)]:

$$L = L_L \frac{1}{1-\frac{2}{9\varepsilon}(\varepsilon-1)^2\frac{\delta}{\alpha}} \quad (11)$$

is enhanced relative to the Lorentz cavity factor if the molecule is more polarizable than the medium. In particular, for $\delta > \frac{9\varepsilon\alpha}{2(\varepsilon-1)^2}$, the theory fails. This regime, known as the Clausius–Mossotti catastrophe, might describe a ferroelectric transition, which corresponds to a spontaneous polarization of the system. The local electric field felt by the probe molecule is enhanced, relative to the macroscopic field, by the local field factor L. The vacuum fluctuations of the electric field, which are responsible for spontaneous emission, are enhanced by the same factor. The spontaneous emission rate Γ_r is thus enhanced by a factor L^2 with respect to the one given in Equation (2): $\Gamma_r = nL^2\Gamma_{r0}$.

In order to apply these considerations in the case of a DiD molecule embedded in a PS matrix, we have calculated the polarizabilities and volumes of the DiD molecule and those of a styrene unit. Firstly, an optimization of the respective geometries has been performed in the ground state by using the semiempirical Hartree–Fock Austin Model 1 (AM1) technique and in the excited state by coupling the AM1 method to a full configuration interaction scheme (CI) within a limited active space, as implemented in the Ampac package.[19] Secondly, the optical absorption spectra of the optimized geometries have been computed by means of the semi-empirical Hartree–Fock intermediate neglect of differential overlap (INDO) method, as parameterized by Zerner et al.,[20] combined to a single configuration interaction (SCI) technique; the CI space is built here by promoting one electron from one of the highest sixty occupied levels to one of the lowest sixty unoccupied ones. Finally, the polarizabilities were determined by a sum over states (SOS) method over all states involved in the CI space just mentioned. Figure 4 shows the optimized geometry of the DiD

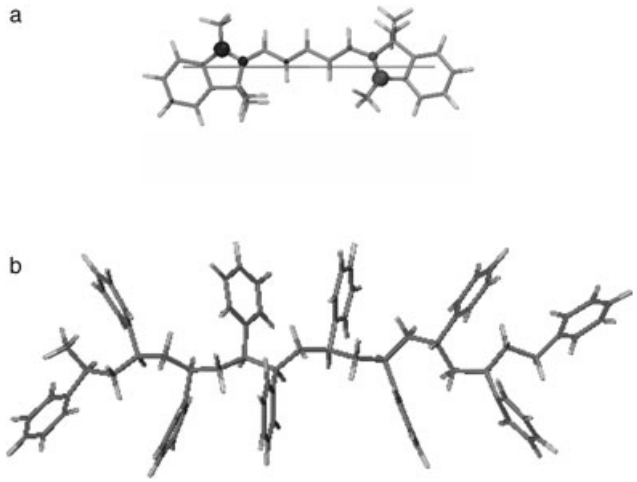

Figure 4. *Schematic structures of the DiD molecule (a) and of a section of the poly(styrene) chain (b). The atomic transition densities and the transition dipole moment associated to the HOMO–LUMO transition are also shown.*

molecule (only the most abundant conformer is shown) and of a section of a PS chain. The atomic transition densities, as well as the transition dipole moment ($|\vec{\mu}| = 4.97\times10^{-29}$ C m) associated to the transition between the ground state and the lowest excited state of the molecule are also shown.

The polarizabilities of the DiD molecule $\chi_0 = 6.1\times10^{-39}\,C^2\,m^2\,J^{-1}$ ($\chi_0 = 55\times10^{-30}4\pi\varepsilon_0\,m^3$) and of the styrene unit $\alpha = 1.0\times10^{-39}\,C^2\,m^2\,J^{-1}$ ($\alpha = 9\times10^{-30}4\pi\varepsilon_0\,m^3$) have thus been determined, as well as their volumes $V = 399\times10^{-30}\,m^3$ and $V = 119\times10^{-30}\,m^3$, respectively. Note that these effective polarizabilities have been averaged over the three tensor axes. As a check, we also deduced the volume V of the styrene unit by use of the Clausius–Mossotti equation [Eq. (10)], knowing the dielectric permittivity of PS ($\varepsilon = 2.5$) and the polarizability α of the unit. The value obtained this way $V = 113\times10^{-30}\,m^3$ is consistent with the volume calculated by quantum chemistry.

In order to determine quantitatively the influence of the polarizability and the spatial extent of the DiD molecule on the spontaneous emission rate of the probe $\Gamma_r = nL^2\Gamma_{r0} = nL_L^2\,\hat{L}^2\Gamma_{r0}$, the ratio $\hat{L}^2 = (\frac{L}{L_L})^2$ was calculated in different cases. This ratio given by Equation (11) in the case of a spherical, polarizable

probe, expresses the departure from the ideal Lorentz behavior, for which $\hat{L}^2=1$. Table 1 (fourth column, first two lines) shows the calculated ratios $\hat{L}^2$ in the case where the probe molecule is represented by a point dipole, which occupies the same volume $V=113\times10^{-30}\,m^3$ as the molecules of the medium (styrene units). Only the polarizability of the molecule changes, and takes, respectively, the values 0 and α, as indicated in the second column of the table. These two cases correspond to the empty and Lorentz cavity factors, respectively. The third line of the table pertains to the case where the probe molecule, with its actual polarizability χ_0, is represented by a point dipole occupying its actual volume $V=399\times10^{-30}\,m^3$.

Table 1. *Ratio $\hat{L}^2$ for the considered three polarizabilities and two spatial extensions of the probe molecule. "Extended" means ellipsoidal cavity in the theory and extended dipole in the simulations.*

Dipole	Polarizability	Shape theory	$\hat{L}^2$ theory	Shape simulation	$\hat{L}^2$ simulation
point	0	spherical	0.694	1 cubic cell	0.814
point	α	spherical	1	1 cubic cell	1
point	χ	spherical	1.369	-	-
"extended"	0	ellipsoidal	0.509	3 aligned cubic cells	0.512
"extended"	3α	ellipsoidal	0.578	3 aligned cubic cells	0.579
"extended"	χ	ellipsoidal	0.667	3 aligned cubic cells	0.771

Table 1 shows clearly that the ratio $\hat{L}^2$ increases as the polarizability of the probe molecule is increased, ranging from a value lower than 1 in the case of the empty cavity model, to 1 in the case of the Lorentz cavity model, and higher than 1 in case the polarizability of the probe molecule is enhanced with respect to the surrounding medium molecules. If the actual polarizability χ_0 of a DiD molecule would have been confined to the small volume of a styrene unit, a Clausius–Mossotti catastrophe would have been generated.

2.3 Effect of the Elongated Shape

In the three cases just mentioned, the probe molecule has been sized to an idealized spherical volume. However, a DiD molecule has an elongated shape (Scheme 1) and occupies a volume $V=399\ 10^{-30}\,m^3$, which is a bit more than three times the volume of a styrene unit. We thus propose to replace a small volume of the medium by an extended dipole in an ellipsoidal cavity with principal semi-axes *aR*, *bR* and *cR* ($a=1$, $b=1$ and $c=3$) along the *x*, *y* and z axes of a Cartesian coordinate system, respectively. In this case the local field factor is given by Equation (12):[18]

$$L=\frac{\varepsilon}{\varepsilon+(1-\varepsilon)A_c-3A_c(1-A_c)(\varepsilon-1)\frac{\chi}{4\pi\varepsilon_0 abcR^3}} \qquad (12)$$

where [Eq. (13)]:

$$A_c=\frac{abc}{2}\int_0^\infty \frac{1}{(s+c^2)\sqrt{(s+a^2)(s+b^2)(s+c^2)}}ds \qquad (13)$$

In the case of a spherical cavity ($a=b=c=1$), $A_c=1/3$, Equation (12) converts back to Equation (9). The calculated values [Eq. (12)] of the ratios $\hat{L}^2$ are given in Table 1 (last three lines) for the three polarizabilities of the probe molecule previously considered: 0, α and χ_0. By using such an extended dipole to represent the single molecule, no catastrophe is generated, as the "real" polarizability of the molecule is confined in a "real" volume. Table 1 shows that a probe molecule represented by an extended dipole has a spontaneous emission rate, which is enhanced as its polarizability is increased. Interestingly, the calculated ratios in the case of the molecule represented by either a point dipole of polarizability $\chi=0$ or a dipole in a ellipsoidal cavity of polarizability $\chi=\chi_0$ are similar, which justifies the approach adopted earlier in the literature.[11]

So far, although the described models are very relevant to calculate the spontaneous emission rate and thus the fluorescence lifetime of a DiD molecule embedded in the PS matrix, none of them is able to explain the lifetime fluctuations observed experimentally. We now consider inhomogeneities of the solvent shells in a microscopic approach, using numerical simulations.

3. Microscopic Lattice Model

An amorphous polymer matrix is a frozen disordered medium that consists of polymer chains and holes. Even 80 K below the glass transition temperature ($T_g=373$ K for PS), the glassy state relaxes as a result of local configuration rearrangements of chain segments, which are described by the hole motion and bond rotation.[21]

3.1 Description of the Model

The probe molecule is represented by a charge distribution $\rho(\vec{r})$ oscillating (for the considered HOMO–LUMO transition) at the transition frequency ω_{eg}. The charge distribution $\rho(\vec{r})$ is related to the transition dipole moment $\vec{\mu}$ of the molecule by the relation $\vec{\mu}=\int\vec{r}\rho(\vec{r})d\vec{r}$. Figure 4a shows an illustration of the atomic transition densities associated with the transition between the ground state and the lowest excited state of the DiD dye (predominantly described as a HOMO to LUMO transition). The arrow describes the orientation of the transition dipole moment $\vec{\mu}$ of the molecule; $|\vec{\mu}|=4.97\times10^{-29}\,C\,m$. The probe molecule is placed at the origin of a three-dimensional cubic lattice and is surrounded by *N* polarizable monomers (Figure 5). In order to mimic the motion of the styrene units around the fixed probe molecule, a given fraction of holes is introduced in the lattice. Figure 4b shows the styrene units of a portion of a poly(styrene) chain that constitutes the matrix. To determine the lattice constant, Δ, the van der Waals volume

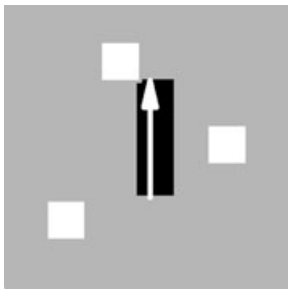

Figure 5. *Two-dimensional representation of a cubic lattice having the probe molecule at the center(black sites), surrounded by the styrene units (gray sites) and some holes (white sites).*

of a styryl unit $V=\Delta^3$ is simply attributed to the volume of a cell of the cubic lattice.

In the study, we represent the probe molecule as an extended dipole of length $l=8.9\times10^{-10}$ m (distance between N atoms) with point charge $q=\frac{|\vec{\mu}|}{l}$. This extended dipole, which closely mimics the transition density distribution in Figure 4, occupies three cells of the cubic lattice (Figure 5). The electric field created by this source dipole on the surrounding polarizable monomers situated at positions $\vec{r}_k$ is $\vec{E}(\vec{r}_k)=-\vec{\nabla}V(\vec{r}_k)$, with [Eq. (14)]:

$$V(\vec{r}_k)=\frac{q}{4\pi\varepsilon_0}\left(\frac{1}{|\vec{r}_k-\vec{r}_+|}-\frac{1}{|\vec{r}_k-\vec{r}_-|}\right) \tag{14}$$

where $\vec{r}_+=(0,0,\frac{l}{2})$ and $\vec{r}_-=(0,0,-\frac{l}{2})$ are the positions of the plus and minus charges of the source dipole, respectively. The case of a point source dipole will also be considered as a special case of the extended dipole with $l\rightarrow0$. In this case, the source dipole only occupies the cell at the origin of the cubic lattice. The dipoles $\vec{\mu}_k$ induced by the electric field on the surrounding monomers, considered as point dipoles, are obtained from the set of coupled Equations (15) and (16):

$$\vec{\mu}_k=\alpha_k\left[\vec{E}(\vec{r}_k)+\sum_{j=1}^{N}\hat{T}_{kj}\vec{\mu}_j)\right] \tag{15}$$

where $\hat{T}_{kj}$ is the dipole–dipole interaction tensor:

$$\hat{T}_{kj}=\frac{1}{r_{kj}^3}\left(\hat{I}-\frac{3\vec{r}_{kj}\vec{r}_{kj}}{\vec{r}_{kj}^2}\right) \tag{16}$$

where $\hat{I}$ is the identity tensor and $\vec{r}_{kj}=\vec{r}_k-\vec{r}_j$. The second term in the set of coupled equations [Eq. (15)] also includes the interactions between the monomers once they have been polarized (polarizabilities $\alpha_k=\alpha$) by the electric field $\vec{E}(\vec{r}_k)=-\vec{\nabla}V(\vec{r}_k)$ [Eq. (14)]. Interactions between polarized monomers and the polarizable probe molecule (polarizability $\alpha_k=\chi$), placed at the origin of the lattice and source of this electric field are also considered in this expression. The local electric field, felt by the probe molecule, is thus the sum of all electric fields experienced by the surrounding monomers and of the reaction field induced by all these polarized monomers that act back on the probe molecule.

We now have treated all interactions within the first solvent shells [see Figure 2, (1)+(2)]). This system has an effective transition dipole moment $\vec{\mu}_{tot}$, which is the sum of the molecular dipole moment (source dipole) $\vec{\mu}$ and of the induced dipoles $\vec{\mu}_k$ of the cubic array representing the solvent shells [Eq. (17)]:

$$\vec{\mu}_{tot}=\vec{\mu}+\sum_k\vec{\mu}_k \tag{17}$$

with $\vec{\mu}_k$ given by Equation (15).

We now embed our system into the continuous dielectric [see Figure 2, (3)] using Lorentz's procedure, which amounts to multiplying by the Lorentz local field factor. The spontaneous emission rate Γ_r of the probe molecule embedded in a heterogeneous disordered medium can thus be written as Equation (18):

$$\Gamma_r=nL_L^2|\frac{\vec{\mu}_{tot}}{\vec{\mu}}|^2\Gamma_{r0} \tag{18}$$

with Γ_{r0} given by Equation (1). The near-field effect of the disordered heterogeneous medium on the radiative lifetime can thus be evaluated completely on the base of electrostatic calculations of the ratio $r=|\frac{\vec{\mu}_{tot}}{\vec{\mu}}|^2$ between the total dipole in the cavity and the source dipole associated with the probe molecular charge distribution. It is worthwhile to note here the equivalence between the ratio $\hat{L}^2$, defined in Sections 2.2–2.3 and expressing the dependence of the polarizability and spatial extent of the probe molecule on its spontaneous emission rate (Table 1) and the ratio $r=|\frac{\vec{\mu}_{tot}}{\vec{\mu}}|^2$ just defined in Equation (18). Liver et al. first showed that a first-order quantum-mechanical perturbation theory of the solvent effect on molecular oscillator strengths is equivalent to the classical electrostatic approach.[22] The ratio $|\frac{\vec{\mu}_{tot}}{\vec{\mu}}|^2$ can be easily evaluated numerically for a disordered system. The results of this investigation are presented in the next subsection.

3.2 Numerical Evaluation of the Oscillator Strengths Ratio—Comparison with the Continuum Approach

As a first step, we consider the interaction of the probe molecule, represented as a point dipole located at the center of a cubic array in vacuum, and a monomer (styrene unit) placed either transversally or longitudinally with respect to the dipole axis of the single probe molecule. Figure 6 shows the computed ratio $r=|\frac{\vec{\mu}_{tot}}{\vec{\mu}}|^2$ as a function of the probe molecule—monomer distance, expressed in units of $\Delta=4.8\,10^{-10}$ m. If the monomer is placed at a large distance with respect to the probe molecule, the ratio is obviously equal to unity (very weak electrostatic interactions). As the distance separating the interacting species is reduced, the ratio is increased (de-

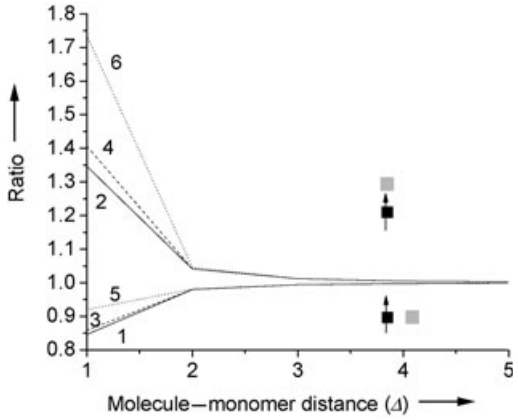

Figure 6. *Ratio* $r = |\frac{\mu_{tot}}{\mu}|^2$ *calculated in the case of a monomer placed transversally (curves 1, 3, 5) or longitudinally (curves 2, 4, 6) with respect to the axis of a point dipole located at the origin of the lattice. The molecule–monomer distance is expressed in units of cell interdistance* $\Delta = 4.8\,10^{-10}$ *m. Curves 1 and 2, 3 and 4, and 5 and 6, pertain to a point dipole with polarizability 0,* α*, and* χ*, respectively.*

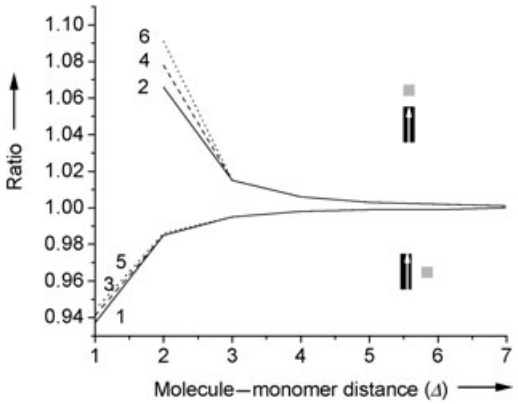

Figure 7. *Ratio* $r = |\frac{\mu_{tot}}{\mu}|^2$ *calculated in the case of a monomer placed transversally (curves 1, 3, 5) or longitudinally (curves 2, 4, 6) with respect to the axis of an extended dipole located at the origin of the lattice. The molecule–monomer distance is expressed in units of cell interdistance* $\Delta = 4.8\,10^{-10}$ *m. Curves 1 and 2, 3 and 4, and 5 and 6, pertain to a point dipole with polarizability 0,* 3α*, and* χ*, respectively.*

creased) in the case of a longitudinally (transversally) located monomer. The increased (decreased) value of the ratio obtained by placing the monomer longitudinally (transversally) with respect to the dipole axis simply results from the vector addition of the induced dipole moment $\vec{\mu}_k$ of the polarizable monomer to the source dipole moment to give the total dipole moment $\vec{\mu}_{tot} = \vec{\mu} + \vec{\mu}_k$.

Three cases are reported in Figure 6, corresponding to three different polarizabilities attributed to the probe molecule: zero for a nonpolarizable molecule (solid lines; ——), α for a probe molecule with the polarizability of a styrene unit (dashed lines; -----) and χ_0 for a molecule with the polarizability of DiD confined to a small volume (dotted lines; •••••). Figure 6 clearly shows that an increase in the polarizability of the probe molecule is accompanied by a corresponding increase in the ratio *r*. As the fluorescence lifetime of a single molecule is the reciprocal of the spontaneous emission rate, the effect of placing a monomer close to the molecule, along the dipole axis, is thus to reduce its lifetime by a factor *r*. This effect can be as drastic as a modification of 35 to 70% of the lifetime, depending on the polarizability of the probe molecule. It is also worth noting that the variation induced by placing a monomer longitudinally with respect to the dipole axis is significantly larger than the one induced by placing the monomer transversally.

In case the probe molecule, placed at the origin of the cubic lattice, is represented by the extended dipole, the effect of the molecule–monomer interaction on the ratio *r*, as a function of the separating distance, is very similar, but attenuated with respect to the case of the point dipole. Figure 7 shows that, in this case, the fluorescence lifetime variations can only reach 6 to 9% of the natural lifetime of the molecule, in the best case that of a longitudinally positioned monomer. The three polarizabilities attributed per cell occupied by the probe molecule are 0, α and $\frac{\chi_0}{3}$, respectively. The polarizability of the DiD molecule has been split equally into three parts, in the last case, assuming it fulfills the additivity property. In each of the three cases, the monomer, which occupies one cell of the lattice, interacts with the three cells occupied by the probe molecule. These three cells occupied by the probe molecule also interact with each other.

Figure 8 shows the computed ratio $r = |\frac{\vec{\mu}_{tot}}{\vec{\mu}}|^2$ as a function of the number of added polarization shells of monomers around the probe molecule on the cubic lattice. Both results for the point dipole and the extended dipole are shown in this Figure. The minimum radiative lifetime (maximum oscillator strength $|\vec{\mu}_{tot}|^2$) is observed with the completion of a full first solvation layer of styrene units around the probe molecule.[23] Adding a second or third layer lengthens the lifetime. The saturation of the probe molecule's lifetime with larger number of styrene units in its vicinity is associated with an approximate continuum dielectric behavior, where Equations (9) and (12) apply in the case of a point dipole and an extended dipole, re-

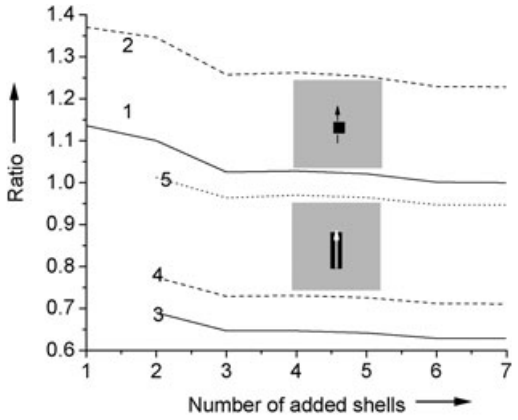

Figure 8. *Ratio* $r = |\frac{\mu_{tot}}{\mu}|^2$ *calculated in case the cubic lattice is filled with several shells of monomers around the probe molecule located at the origin of the lattice. Curves 1 and 2 pertain to the probe molecule represented as a point dipole with polarizability 0 and* α*, respectively. Curves 3, 4 and 5 pertain to the probe molecule represented as an extended dipole with polarizability 0,* 3α *and* χ*, respectively.*

spectively. It is remarkable that the approximate continuum behavior is reached only after a few (actually six) solvation shells have been added to the probe molecule. Very interestingly, Figure 6 and Figure 7 show that curves 2, 4 and 6 (curves 1, 3, 5) join already as an interdistance of 2Δ separates the molecule from the monomer placed longitudinally (transversally) with respect to the dipole axis of the molecule: the influence of the molecular polarizability vanishes rapidly with an increase of the molecule–monomer interdistance. In both cases, two terms can be considered to contribute to the effective dipole moment [Eq. 17)]: 1) The source dipole of the molecule polarizes the surrounding monomer (direct mechanism), a process that scales as the reciprocal of the third power of the distance separating the source dipole and the dipole induced on the monomer [Eq. (16)]; 2) Due to the reaction field of the monomer on the probe molecule, a consecutive forwards (molecule→monomer)–backwards (monomer→molecule) dipole–dipole interaction mechanism leads to a weak interaction (scaling as the reciprocal of the sixth power) for long interdistances between the two species. This forwards–backwards mechanism can thus not compete with the direct mechanism for long interdistances between the molecule and the considered monomer. On the contrary, Figure 8 shows well separated curves, as shells of monomers are added around the probe molecule. In this case, a number of terms, growing as the third power of the cluster radius (each term being proportional to the inverse of the sixth power of the interdistance between the molecule and the monomer of a given shell), sum to give a significant contribution of the forwards–backwards mechanism to the effective dipole moment $\vec{\mu}_{tot}$ [Eq. (17)].

Once the saturation value of the ratio r is reached, after having filled the lattice with successive polarization shells, an approximate continuum dielectric behavior is attained (Figure 2). The numerical calculation of the ratios $\hat{L}^2 = \frac{L^2}{L_L^2}$ may then be compared with the results of the continuum theories [Eqs. (9) and (12)]. At this point, note that curve 2 in Figure 8 reaches a ratio $r = 1.23$ instead of the ratio $r = 1$ which is expected in the case of the ideal Lorentz behavior. We attribute this discrepancy to several possible factors: 1) We use polarizabilities averaged on the three tensor axes. While being very satisfactory in the case of a styrene unit, this approximation is probably not fully appropriate in the case of the elongated DiD molecule; 2) The lattice constant Δ is defined in our microscopic model as $\Delta = V^{1/3}$ (cubic cells), while continuum theories consider spherical molecules, with $V = \frac{4}{3}\pi R^3$ such that $\Delta = 2R$. For obvious packing reasons, we preferred to choose cubic cells instead of spherical ones. Doing so, we have reduced the lattice constant and thus enhanced the dipole–dipole interactions between neighboring cells. This in turn increases the ratio r.

Prior to perform the comparison between our microscopic results and the continuum theories, we thus normalized the different curves shown in Figure 8 with respect to the ideal Lorentz behavior. Table 1 provides the comparisons for each of the considered cases, obtained after renormalization of the curves by a factor 1.23. The matching of the values obtained by theory and by numerical calculations is very good.

3.3 Numerical Evaluation of the Oscillator Strengths Ratio—Effects of the Holes

In order to simulate the mobility of the chain segments surrounding the probe molecule, holes are introduced in the lattice. Figure 9 shows the influence on the ratio $r = |\frac{\vec{\mu}_{tot}}{\vec{\mu}}|^2$ of a

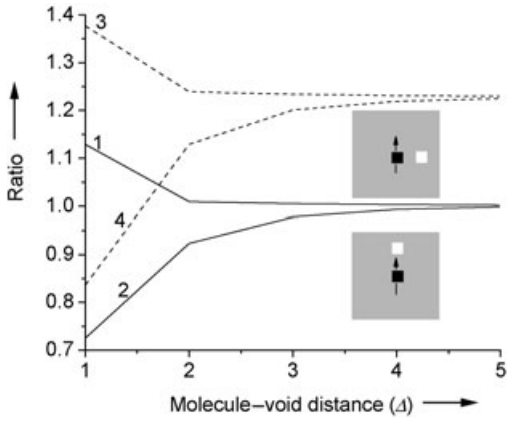

Figure 9. *The cubic lattice is filled with seven shells of polarizable monomers, surrounding the point dipole located at the origin. The ratio* $r = |\frac{\mu_{tot}}{\mu}|^2$ *is calculated in the case of a void placed transversally (curves 1, 3) or longitudinally (curves 2, 4) with respect to the axis of the point dipole. The molecule–void distance is expressed in units of cell interdistance* $\Delta = 4.8\,10^{-10}$ *m. Curves 1 and 2, 3 and 4, pertain to a point dipole with polarizability 0,* α*, respectively.*

void (site of polarizability zero) that approaches the point dipole transversally with respect to its axis, from the continuum to the position just on the right of the source dipole (curves 1 and 3). If this void is added far away from the dipole, its presence has no effect on the radiative lifetime of the probe molecule. The ratio is identical to the one in the absence of the void. On the contrary, as the void approaches the molecule, the ratio r is considerably enhanced. A simple explanation of this effect is the following: the dipole moments induced on the monomer placed transversally with respect to the dipole axis of the probe molecule are opposite to the inducing molecular dipole, and thus add destructively to it. Replacing a monomer by a void at those positions reduces this negative contribution and thus increases the total dipole moment.

Conversely, by putting such a void in a lattice site along the dipole axis of the probe molecule, and approaching it step by step till it reaches the top of the positive charge of the source dipole, the spontaneous emission rate is decreased (curves 2 and 4). These effects are further enhanced if the polarizability of the probe molecule is increased from zero (curves 1 and 2) to α (curves 3 and 4).

Similar effects are observed in case an extended dipole is placed at the origin of the cubic lattice. In this case however, the variations of the ratios are attenuated with respect to the previous case of the point dipole (Figure 10). The maximum lifetime increase, obtained by placing a void close to the molecule with polarizability χ_0 and along its dipole axis, is 11.5%

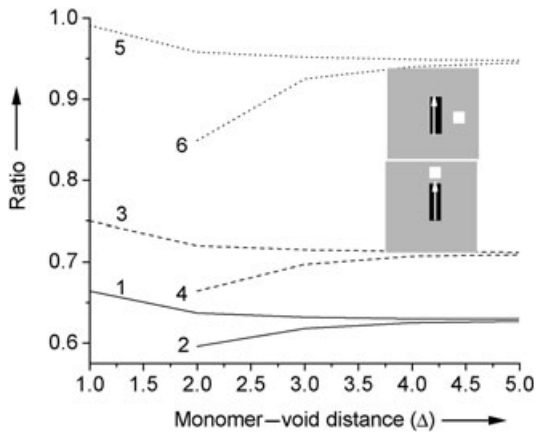

Figure 10. *The cubic lattice is filled with seven shells of polarizable monomers, surrounding the extended dipole located at the origin. The ratio is calculated in the case of a void placed transversally (curves 1, 3, 5) or longitudinally (curves 2, 4, 6) with respect to the axis of the extended dipole. The molecule–void distance is expressed in units of cell interdistance* $\Delta = 4.8\,10^{-10}$ *m. Curves 1 and 2, 3 and 4, and 5 and 6 pertain to an extended dipole with polarizability 0,* 3α*, and* χ*, respectively.*

(curve 6). In case the void is placed close to the molecule on an axis perpendicular to the dipole axis, the maximum lifetime decrease is 4.4% of the natural lifetime of the probe molecule (curve 5).

It is interesting here to compare the results obtained in Figure 10 with those displayed in Figure 7. Figure 7 indeed shows that, not only by placing a monomer longitudinally (curves 2, 4, 6) but also (although less significantly) transversally (curves 1, 3, 5) with respect to the dipole axis of the molecule, the ratio r is increased as the polarizability of the molecule is increased from 0 to χ_0, at short molecule–monomer interdistances. The forwards–backwards mechanism always give a positive contribution to the sum in Equation (17). On the contrary, the direct polarization mechanism gives a positive (negative) contribution to the right hand side of Equation (17), in case the monomer is placed longitudinally (transversally) with respect to the dipole axis of the molecule. As a consequence, the two terms add constructively (destructively), increasing significantly (slightly) the ratio r, in case a monomer is placed longitudinally (transversally).

These effects are similarly responsible for the rather high increase of the lifetime (11.5%) once a void is placed close to the molecule with polarizability χ_0 and along its dipole axis (Figure 10) as compared to the transversal case (4.4%) and give a clear explanation to the observation of signicant positive excursions in the fluorescence-lifetime time trace of a single molecule embedded in a PS matrix (Figure 1) as due to the presence of hole(s) positioned close to the molecule and along its dipole axis.

3.4 Numerical Evaluation of the Fluorescence Lifetimes—Monte Carlo Simulations

As a last step, in order to build a distribution of the ratios r or, equivalently, a distribution of the fluorescence lifetimes of a DiD molecule embedded in a PS matrix, we have finally performed a Monte Carlo simulation of the actual configuration of the molecule with polarizability $\chi = 6.1\times10^{-39}\,C^2\,m^2\,J^{-1}$ and volume $V = 399\times10^{-30}\,m^3$ spread over three cubic cells of the lattice and surrounded by styrene units and holes. A Monte Carlo run is implemented in the following way: 1) We specify the fraction of holes (threshold value) that will be present in the system; 2) For each cell on the lattice, a uniformly distributed (between zero and one) random number is chosen; 3) If the random number falls below the threshold value, then the given cell is occupied by a hole, else the cell is occupied by a monomer. The complete Monte Carlo simulation involves 1000 runs for each given threshold value.

Figure 11a shows the result of such a Monte Carlo simulation in the case of a hole fraction $h = 6\%$. Remarkably the fluorescence lifetime shows peaks towards higher values, which results from configurations with holes localized longitudinally with respect to the source dipole axis. The histogram of the calculated fluorescence lifetimes is asymmetric and shows de-

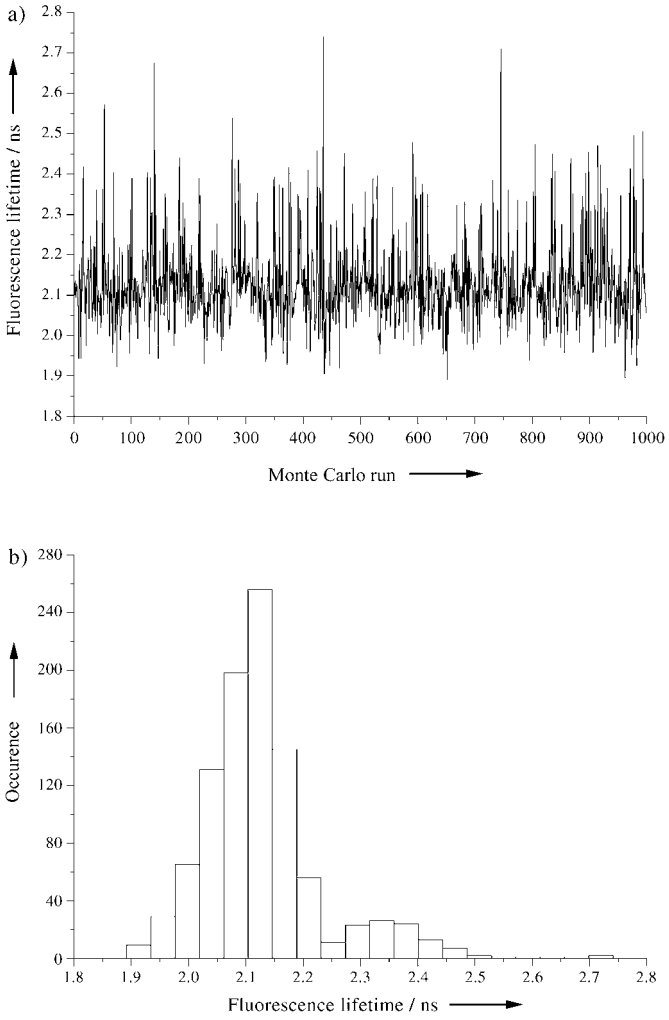

Figure 11. *Fluorescence lifetime calculations (a) and corresponding distribution for a Monte Carlo run of 1000 steps. The cubic lattice is here filled with six shells of polarizable monomers surrounding the extended dipole of polarizability* χ*, located at the origin. Holes are placed at random positions on the lattice with a fraction* $h = 6\%$*.*

viations reaching 30% of the average lifetime, in a very similar way as the experimental results shown in Figure 1. The two maxima in the histogram (Figure 11 b) for long lifetimes are due to the discreteness of the lattice and correspond to voids positioned against the molecule for the bunch observed around 2.7, one site away from it for the bunch at 2.35.

Figure 12 shows the same results in case a fraction $h=1\%$ (a), $h=10\%$ (b), $h=20\%$ (c) and $h=40\%$ (d) of holes is introduced in the system. Figure 12 clearly shows that, by increasing the fraction of holes present in the system, the fluorescence lifetime distribution gets broadened and asymmetric. For a hole fraction $h=1\%$, the lifetime distribution is very narrow and mainly symmetrical. If the local environment of the probe molecule is composed of a $h=10\%$ fraction of holes (which is a typical amount in a polymer matrix[24]), the distribution gets asymmetric towards higher lifetimes. This result is in very good agreement with the experimental results, reported by Vallee et al.,[11] that the asymmetry of the fluorescence lifetime distributions increases as the temperature of the PS matrix is raised: the fraction of holes present in a matrix is indeed an increasing function of the temperature.

As the hole fraction still increases above $h=10\%$, the lifetime distribution becomes mainly broadened, while keeping its asymmetry (Figures 12 c and 12 d).

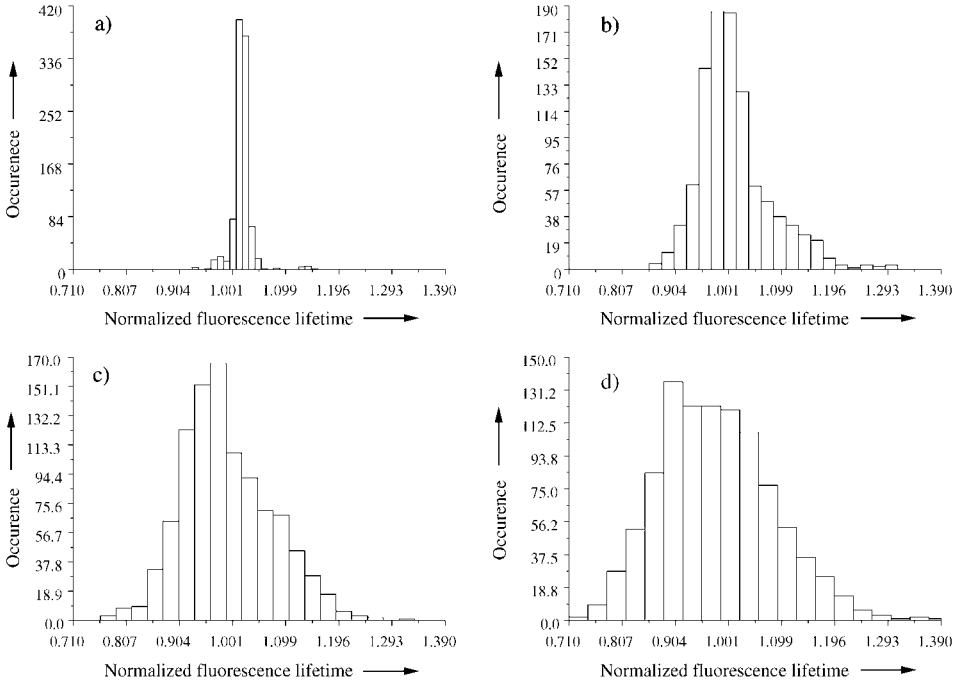

Figure 12. *Fluorescence lifetime distributions for Monte Carlo runs of 1000 steps. The cubic lattice is filled with six shells of polarizable monomers surrounding the extended dipole of polarizability χ, located at the origin. Holes are placed at a random positions on the lattice with a fraction* h = *1% (a),* h = *10% (b),* h = *20% (c),* h = *40% (d).*

4. Conclusions

A microscopic model has been developed to account for the observed temporal lifetime fluctuations of a single DiD molecule embedded in a poly(styrene) matrix at room temperature. The model is based on the description of the system as a cubic lattice with sites that can accommodate the repeating units of a macromolecule, the probe molecule, and some voids to account for the mobility of the matrix. The probe molecule has been represented as a point dipole or as an extended dipole with different values of the polarizability. Firstly, the model has been validated, by comparing its approximate continuum dielectric behavior to existing theories. Secondly, we have shown that the observed asymmetry of lifetime variations towards higher values very probably results from positional fluctuations of voids close to the extremities of the extended dipole representing the probe molecule. Thirdly, Monte Carlo simulations have been performed successively to describe such systems possessing a different but fixed fraction h of holes. The calculated radiative lifetime distributions have been shown to be more and more broadened and asymmetric as the fraction h of holes present in the system is increased. This behavior is in excellent agreement with the one experimentally observed by Vallée et al.[11] As such, the approach considered in this paper is a first attempt to describe the effect of the local, near field on the behavior of a probe molecule. This type of approach is only possible with the advent of single-molecule spectroscopy that allows to perform such detailed investigations.

Acknowledgements

R. A. L. Vallée thanks the FWO for a postdoctoral fellowship. D. Beljonne is a research associate of the FNRS. The authors are grateful to the University Research Fund, the Federal Science Policy through the IAP/V/03, and the FWO, for supporting this research project.

Keywords: dielectric properties · local field · luminescence · polymers · single-molecule studies

[1] D. P. Craig, T. Thirunamachandran, *Molecular Quantum Electrodynamics: An Introduction to Radiation–Molecule Interactions*, Academic Press, London **1984**.
[2] R. J. Glauber, M. Lewenstein, *Phys. Rev. A* **1991**, *43*, 467.
[3] A. Lagendijk, B. Nienhuis, B. A. van Tiggelen, P. de Vries, *Phys. Rev. lett.* **1997**, *79*, 657.
[4] E. Yablonovitch, T. J. Gmitter, R. Bhat, *Phys. Rev. Lett.* **1988**, *61*, 2546.

[5] P. de Vries, A. Lagendijk, *Phys. Rev. Lett.* **1998**, *81*, 1381.
[6] M. F. Perutz, *Science* **1978**, *201*, 1187.
[7] A. Warshel, S. T. Russell, *Q. Rev. Biophys.* **1984**, *17*, 283.
[8] Xueyu Song, *J. Chem. Phys.* **2002**, *116*, 9359.
[9] W. E. Moerner, M. Orrit, *Science* **1999**, *283*, 1670.
[10] E. A. Donley, T. Plakhotnik, *J. Chem. Phys.* **2001**, *114*, 9993.
[11] R. A. L. Vallée, N. Tomczak, L. Kuipers, G. J. Vancso, N. F. van Hulst, *Phys. Rev. Lett.* **2003**, *91*, 038 301.
[12] R. Simha, T. Somcynski, *Macromolecules* **1969**, *2*, 342.
[13] R. Simha, *Macromolecules* **1977**, *10*, 1025.
[14] D. E. Aspnes, *Am. J. Phys.* **1982**, *50*, 704.
[15] F. J. P. Schuurmans, P. de Vries, A. Lagendijk, *Phys. Lett. A* **2000**, *264*, 472.
[16] R. A. L. Vallée, G. J. Vancso, N. F. van Hulst, J.-P. Calbert, J. Cornil, J. L. Brédas, *Chem. Phys. Lett.* **2003**, *372*, 282.
[17] G. Nienhuis, C. Th. J. Alkemade, *Physica B+C* **1976**, *81*, 181.
[18] C. J. F. Böttcher, *Theory of electric polarization, Vol.* 1, *2nd ed.*, Elsevier, Amsterdam, **1973**.
[19] AMPAC Semichem, 7204 Mullen, Shawnee, KS 66 216.
[20] M. C. Zerner, G. H. Loew, R. Kichner, U. T. Mueller-Westerhoff, *J. Am. Chem. Soc.* **2000**, *122*, 3015.
[21] T. S. Chow, *Mesoscopic Physics of Complex Materials*, Springer, New York, **2000**.
[22] N. Liver, A. Nitzan, A. Amirav, J. Jortner, *J. Chem. Phys.* **1988**, *88*, 3516.
[23] J. Gersten, A. Nitzan, *J. Chem. Phys.* **1991**, *95*, 686.
[24] R. E. Robertson, R. Simha, J. G. Curro, *Macromolecules* **1984**, *17*, 911.

Received: September 16, 2004

